Toward goal-oriented robotic gait training: the effect of gait speed and stride length on lower extremity joint torques

Robert L. McGrath[1*], Margaret Pires-Fernandes[1,2*], Brian Knarr[3], Jill S. Higginson[4,1], and Fabrizio Sergi[1,4]

***Abstract*— Robot-assisted gait training is becoming increasingly common to support recovery of walking function after neurological injury. How to formulate controllers capable of promoting desired features in gait, i.e. goals, is complicated by the limited understanding of the human response to robotic input. A possible method to formulate controllers for goal-oriented gait training is based on the analysis of the joint torques applied by healthy subjects to modulate such goals. The objective of this work is to understand how sagittal plane joint torque is affected by two important gait parameters: gait speed (GS) and stride length (SL). We here present the results obtained from healthy subjects walking on a treadmill at different speeds, and asked to modulate stride length via visual feedback. Via principal component analysis, we extracted the global effects of the two factors on the peak-to-peak amplitude of joint torques. Next, we used a torque pulse approximation analysis to determine optimal timing and amplitude of torque pulses that approximate the SL-specific difference in joint torque profiles measured at different values of GS. Our results show a strong effect of GS on the torque profiles in all joints considered. In contrast, SL mostly affects the torque produced at the knee joint at early and late stance, with smaller effects on the hip and ankle joints. Our analysis generated a set of torque assistance profiles that can be experimentally tested using gait training robots.**

I. INTRODUCTION

Stroke is a leading cause of long-term disability, with roughly 30% of survivors requiring walking assistance [1]. Current approaches to gait training are based on repetitive movement exercise. Most gait rehabilitation protocols are focused on increasing self-selected gait speed (ss-GS), as it is a powerful indicator of walking function [2]. Walking speed is correlated with propulsive force at push off [3], which is mostly determined by ankle moment and by the posture of the trailing limb at push-off [4]. Push-off leg posture can be described by the trailing limb angle (TLA), i.e. the angle between the vertical axis and the vector between the hip joint and the center of pressure at the instant of maximum anterior ground reaction force. TLA was shown to be highly correlated to propulsive forces during locomotion in both healthy and post-stroke individuals [4]. Although a relationship between TLA and propulsive forces has been determined, the clinical significance of this observation for post-stroke gait training has yet to be demonstrated.

Robot-aided gait training has been pursued in neurorehabilitation since the mid-90s, with initial attempts providing non-convincing results [5]. While the initial approaches lacked interaction control capabilities, later work presented assistance schemes based on the Assist-As-Needed (AAN) principle [6]–[8]. To provide adaptability, algorithms for desired trajectory definition have been proposed based on walking speed [9], and also included on-line assistance adaptation schemes based on adaptive frequency oscillators [10], or inter-limb synchronization [11]. Proper implementation of controllers for continuous gait assistance requires explicit estimation of gait cycle phase, difficult to predict reliably [12], or phase locking with synchronous kinematic variables, which are however associated with the gait cycle phase with substantial within-subject variability [13]. Simpler assistance schemes, such as those provided by repetitive pulses of torque applied to lower extremity joints, have the advantage of not constraining gait to follow prescribed trajectories, while inducing desirable effects such as entrainment and modulation of spatio-temporal gait parameters [14]. Being defined by a limited set of parameters, these approaches are amenable to systematic experimental investigations to determine when and how to apply pulses of torque to effectively modulate clinically meaningful gait parameters.

Given the clinical relevance of ss-GS, and the mechanistic relationship between GS and TLA, a gait training controller

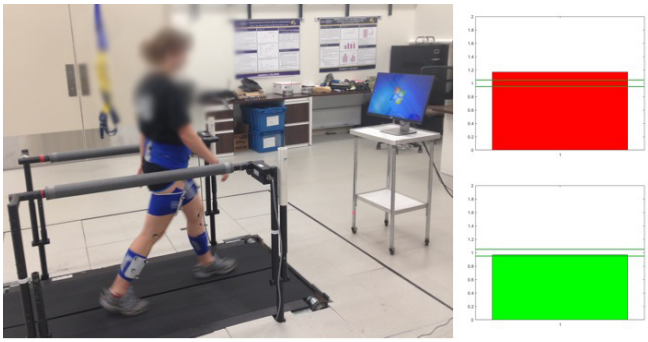

Fig. 1. (left) Experimental setup - shown in ss-GS, ss-SL conditions, and (right) visual feedback modes indicating color coding of measured SL (green indicates SL within 10% of the desired value).

This work was supported by the NSF-CBET-1638007, the NSF-REU-1460757, and the NIH 1 P30 GM103333-01

[1] Department of Biomedical Engineering, University of Delaware, Newark, DE 19713, USA

[2]Department of Biomedical Engineering, University of Florida, Gainesville, FL 32611, USA

[3]Department of Biomechanics, University of Nebraska, Omaha, NE 68182, USA

[4]Department of Mechanical Engineering, University of Delaware, Newark, DE 19713 USA

[*] Equal contribution

capable of directly modulating TLA could have a high clinical value in neurorehabilitation. To formulate TLA-oriented robot-assisted training, we seek to gain knowledge about the joint torques applied by healthy subjects walking at different gait speeds to modulate TLA. Using a robot to apply the torque used by healthy subjects to modulate TLA during gait might be an effective method to modulate TLA in individuals who may retain this gait characteristic, and ultimately improve walking function. As a first step in our approach to goal-oriented, robot-assisted gait training, in this paper, we study the effect of a factorial modulation of gait speed (GS) and stride length (SL) on the resulting moments about the hip, knee and ankle joint in healthy subjects.

II. METHODS

A. Subjects

Ten healthy adults (6 males, 4 females), naive to the purpose of the study, participated in the experiment. All subjects — age (mean $\pm$ std) 21$\pm$ 2 yo, height 1750$\pm$90 mm, body mass 70$\pm$11 kg — were free of orthopaedic and neurological disorders affecting walking function. The experimental protocol was approved by the University of Delaware IRB, and all subjects gave informed consent. Subjects were required to wear their own comfortable sneakers and lightweight athletic gear for the walking experiment.

B. Setup

Subjects walked on an instrumented split-belt treadmill (Bertec Corp., Columbus OH, USA), while wearing reflective spherical markers (diameter 9.5 mm). A total of 36 markers (4 on the pelvis, 4 on each thigh, 4 on each shank, 2 on each knee, and 6 on each ankle/foot) were placed on body segments anatomical landmarks. An eight camera Raptor-4 passive motion capture system (Motion Analysis Corp., Santa Rosa CA, USA) was used to measure the 3D position of markers in space. Marker data were acquired at 100 Hz, while the analog force/torque data were synchronously acquired at 2000 Hz. In biofeedback sessions, subjects walked while watching a 24-in screen placed at approximately 1.5 m distance from the center of the treadmill. The screen provided visual feedback about the stride length (SL) at the previous gait cycle, and was updated immediately after each right heel strike. In this experiment, SL for cycle k was defined based on the anteroposterior (AP) coordinate of right heel strike in the lab frame x_H, accounting for the treadmill constant velocity v_t and for the displacement introduced in a gait cycle of duration ΔT:

$$\mathrm{SL}^{(k)} = x_H^{(k+1)} - x_H^{(k)} + v_t \Delta T \qquad (1)$$

Visual feedback of the most recent SL value was provided in terms of the height of a bar. The desired SL was displayed as a horizontal line with dashed lines indicating $\pm$ 10 % of the desired value. The bar indicating measured SL was color coded to indicate whether $\mathrm{SL}^{(k)}$ was within the $\pm 10\%$ range (Fig. 1). During biofeedback sessions, subjects were instructed to modify their SL to achieve the target range, while walking at treadmill-imposed speeds.

C. Experimental procedures

We exposed subjects to a total of fifteen experimental conditions, determined as the combinations of two factors: *i)* gait speed (GS), with five conditions, and *ii)* stride length (SL), with three conditions. To account for inter-subject variability in gait parameters, and for the correlation between GS and SL [15], we defined factors of all conditions (i.e. values of GS and SL) as percent variation relative to subject-specific self-selected (ss) parameters.

1) Self-selected speed: A preliminary trial was conducted to calculate the subject's self-selected speed (ss-GS). Subjects were asked to walk on the treadmill moving initially at low speed, with the treadmill speed gradually increased by 0.03 m/s, and to indicate when ss-GS was reached. The same procedure was repeated by starting with treadmill speed 0.4 m/s above the previous value, and decreasing treadmill speed in steps of 0.03 m/s, until subjects would indicate that ss-GS had been reached. ss-GS was defined as the average between the two values defined above.

2) Non-biofeedback conditions: After determination of ss-GS, five walking trials were conducted in the absence of biofeedback. In each trial, treadmill speed was imposed at [80% 90% 100% 110% 120%] of the subject ss-GS, with order randomized for each subject. For each GS, self-selected SL (ss-SL) was calculated as the average of SL values measured at each treadmill speed. ss-SL values measured at each speed were used for the definition of subsequent desired SL values at each GS.

3) Biofeedback conditions: After determination of ss-SL for all five GS conditions, ten additional trials were conducted, two for each treadmill speed value, using biofeedback to cue a desired SL. For each GS, the desired SL was set to be either 17% greater or 17% smaller than the ss-SL at that GS, with random sequence. Each trial lasted for approximately two minutes. When the experimenter assessed that the subject could comply with the protocol and match the cued SL condition at each gait speed, data collection was initiated. Data collection lasted for approximately 2 minutes per trial, allowing a measurement of a minimum of 25 strides for each experimental condition and each subject.

D. Data analysis

1) Pre-processing: Marker position and force plate data were fed into a standard Visual3D pre-processing pipeline, which included *i)* low-pass filtering of marker and force plate data (Butterworth filter at 6 Hz and 30 Hz cut-off frequency, respectively), *ii)* interpolation of missing marker data with a third order polynomial fit for a maximum gap size of five samples, *iii)* application of the subject-specific model for calculation of joint angles and moments based on inverse kinematics and inverse dynamics algorithms, *iv)* low-pass filtering of extracted joint angles and moments with a 2nd order low-pass zero-shift Butterworth filter with cut-off frequency of 15 Hz. Hip, knee, and ankle joint angles and moments for the right leg in the sagittal plane were extracted, and gait cycles segmented between subsequent heel strike events, defined as the instant where the vertical ground force

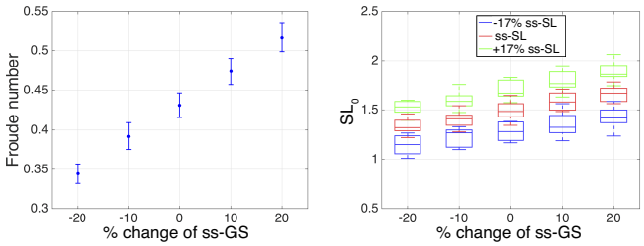

Fig. 2. (left) Distribution of Froude numbers at the different treadmill imposed GS, referred to ss-GS. Whiskers extend to the 95% estimated confidence interval. (right) Normalized stride lengths (SL_0 measured at different speeds, and different biofeedback conditions. The box plot shows the median as a horizontal line, and the box at 25% and 75% percentiles, with whiskers extending to $\pm 3\sigma$.

exceeded a threshold of 20 N and remained above this threshold for at least 400 ms. Because events such as marker occlusion or stepping on both force plates occurred in some cases, acquired data were manually screened and some gait cycles were excluded from the analysis. A minimum of 25 gait cycles per subject, for each experimental condition, were obtained with this procedure.

Joint torques extracted via inverse dynamics were non-dimensionalized for subsequent group analysis. In agreement with [16], the non-dimensional joint torque $\tilde{\tau}$ was calculated for each joint as $\tilde{\tau}(t) = \frac{\tau(t)}{WL_l}$, with τ the measured joint torque in N·m, W is body weight in N, and L_l is leg length, measured from the hip joint center and the malleolus with a straight knee.

Segmented profiles for hip, knee, and ankle joint angles and non-dimensional moments were linearly resampled in the [0,100] domain for synchronization with the gait cycle percentage variable ($\tilde{t}$). Finally, subject- and condition- specific average joint torque profiles $\bar{\tau}(\tilde{t})$ were calculated by averaging all of the available single-stride profiles for each experimental condition, and subject. The resulting profiles underwent statistical analysis and inference via two different methods, as described in the following sections. Because of malfunctioning of the force plate during several sessions involving Subject 9, all kinetics collected from Subject 9 were discarded, leaving effectively N=9 in subsequent statistical analyses.

2) Protocol validation: A non-dimensional GS was defined as the Froude number $Fr = \frac{\text{GS}}{\sqrt{Lg}}$, where L is a representative length, and g is the acceleration of gravity. In this work, L corresponds to the leg length L_l. Although several other factors such as body mass and athletic fitness condition account for the variability in ss-GS across individuals [17], the Froude number has been extensively used to describe the conditions underlying the transition from walking to running in several species [18]. As such, we used the Froude number as an index of across-subject dynamic similarity in ss-GS: a smaller variance of Froude numbers within a group of individuals should reflect consistent gait kinetics. We calculated the coefficient of variation $CV_{Fr} = \frac{\sigma_{Fr}}{\mu_{Fr}}$ as the ratio between the standard deviation and the mean of Froude numbers corresponding to the ss-GS condition, and compared it to alternative indices, $CV_{\text{ss-GS}} = \frac{\sigma_{\text{ss-GS}}}{\mu_{\text{ss-GS}}}$ that uses ss-GS, and $CV_{\text{ss-GS}_0} = \frac{\sigma_{\text{ss-GS}_0}}{\mu_{\text{ss-GS}_0}}$ that uses ss-GS normalized by leg length.

Two gait parameters were also calculated; SL was measured using eq. (1), while the trailing limb angle (TLA) was calculated as the angle relative to the vertical axis of the line connecting the hip joint center and the position of the center of pressure at the instant of maximum anterior ground reaction force [4]. We conducted a linear correlation between normalized SL ($\text{SL}_0 = \text{SL}/L_l$) and TLA to validate our protocol as suitable to inform the design of TLA-oriented robot-aided training protocols.

3) PCA analysis: We sought to determine whether the effect of the two factors, GS and SL, on the resulting joint torque profiles $\bar{\tau}(\tilde{t})$ was that of proportionally scaling and translating along the vertical axis a constant, nominal profile. As such, we used principal component analysis (PCA) to decompose the fifteen subject-specific joint torque profiles $\bar{\tau}_i(\tilde{t})$, $i = 1, 2, ..., 15$, into a sum of fifteen principal components $P_j(\tilde{t})$, each explaining a progressively smaller amount of variance in the input signal, as:

$$\bar{\tau}_i(\tilde{t}) = \sum_{j=1}^{15} a_{ij} P_j(\tilde{t}) + b_i \tag{2}$$

Since the first principal component $P_1(\tilde{t})$ explained more than 95% of the variance in $\bar{\tau}_i(\tilde{t})$ for all joints and all subjects, only coefficients a_{i1} have been used for statistical analysis. Since the arbitrary scaling of a coefficients extracted by PCA would prevent across-subject comparisons, we obtained normalized $\tilde{a}$ coefficients as follows:

$$\tilde{a}_i = a_{i1} \frac{\max[P_1(\tilde{t})] - \min[P_1(\tilde{t})]}{\max[\bar{\tau}_8(\tilde{t})] - \min[\bar{\tau}_8(\tilde{t})]}, \tag{3}$$

where 8 is the index corresponding to the ss-GS, ss-SL condition. Since the term in the numerator describes the peak-to-peak signal of the first principal component, while the term in the denominator describes the peak-to-peak joint torque in self-selected condition, coefficients $\tilde{a}_i$ quantify the ratio of the peak-to-peak variation of the offset-removed approximated signal $\bar{\tau}_{i1}(\tilde{t}) = a_{i1} P_1(\tilde{t})$, for condition i, relative to the self-selected condition.

The coefficients $\tilde{a}_i$ extracted for all joints and all subjects were used as input to three 2-way repeated measures ANOVA tests, one per joint, implemented using SPSS (Ver. 24.0, IBM), which tested the null hypothesis of no significant effect of either factor, nor of their interaction, on PCA scores $\tilde{a}_i$. The two factors, GS and SL were exhaustively spanned with only one repetition of factor combination per subject. Since data collected from Subject 2 in one condition were corrupt, the missing coefficient was replaced by the mean coefficient measured for the same condition in the other 8 subjects. Post-hoc pairwise comparisons between scores extracted in modulated SL conditions and scores extracted in ss-SL conditions were conducted, at each speed, using two-tailed t-tests assuming a type-I error rate $\alpha = 0.05$, corrected for multiple comparisons using a conservative Bonferroni correction.

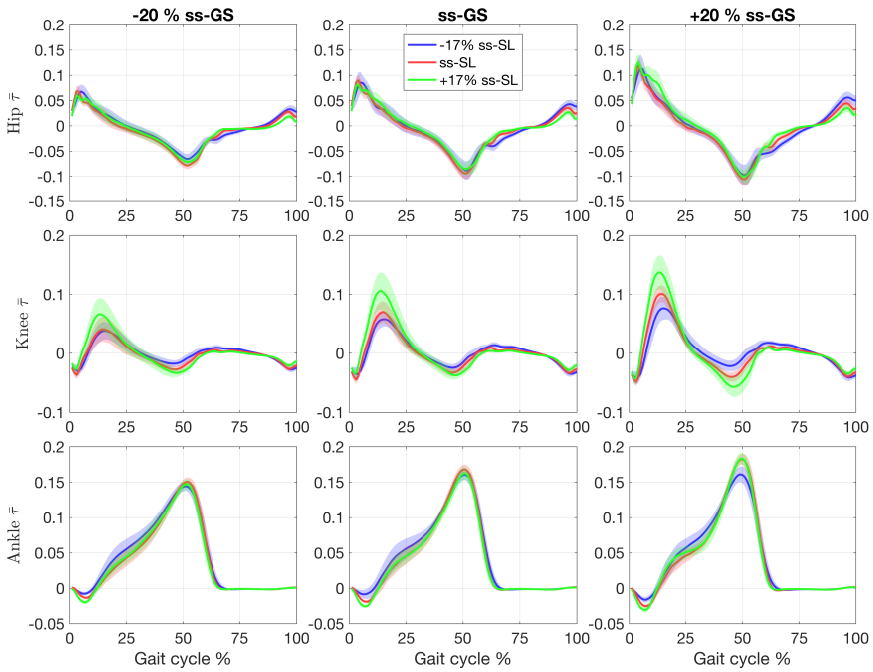

Fig. 3. Effect of gait speed (GS) and stride length (SL) modulation on the normalized joint torques $\bar{\tau}$ for the group of 9 healthy subjects. Joints are organized by row, GS are organized by columns, relative to the subject-specific ss-GS. Conditions corresponding to cued SL values are superimposed on each plot. Lines indicate the group mean, with the shaded region indicating the group standard deviation. Two GS conditions (i.e. GS=$\pm$10% of ssGS) are not reported for clarity of representation.

4) Torque pulse approximation: We sought to approximate the effect of modulation of SL on joint torque profiles with a series of N rectangular torque pulses $P(\tilde{t})$ defined as:

$$Q(\tilde{t}) = \sum_{l=1}^{N} A_l \text{rect}\left(\frac{\tilde{t} - \alpha_l}{0.1}\right) \tag{4}$$

with constant duration (10% of the gait cycle) and variable time of application α_l and amplitude A_l. Specifically, we extracted the difference $\Delta\tau(\tilde{t})$ of average joint torque profiles $\bar{\tau}(\tilde{t})$ between conditions at increased SL, and ss SL, at each gait speed j as:

$$\Delta\tau^{(j)}(\tilde{t}) = \bar{\tau}^{(j)}_{+\text{SL}}(\tilde{t}) - \bar{\tau}^{(j)}_{\text{ss-SL}}(\tilde{t}). \tag{5}$$

For this specific work, we approximated the function $\Delta\tau^{(j)}(\tilde{t})$ with only one pulse $N = 1$, and used nonlinear constrained optimization using MatLab (The MathWorks, Inc.) function `fmincon` to find the values of parameters A_1 and α_1 that minimize the norm of residuals $Q(\tilde{t}) - \Delta\tau$. The set of parameters A_1 measured for different gait speeds and subjects across different joints (i.e. three groups, one per joint, with each group including 45 measurements) underwent pairwise t-tests to test the null hypothesis that the distribution of normalized torque pulse amplitude in different joints had the same mean. Moreover, we sought to quantify how narrow was the distribution of the optimal pulse location α_1 in different joints. As such, we performed three separate pairwise Levene's tests for equality of variances to test the null hypothesis that parameters α_1 in different joints are sampled from distributions with equal variances.

III. RESULTS

A. Protocol validation

The use of the Froude number slightly reduced the across-subject variability in ss-GS, with $CV_{Fr} = 0.048$, smaller than $CV_{\text{ss-GS}} = 0.057$, and $CV_{\text{ss-GS}_0} = 0.059$. All differences account for an effect size that can be considered very small.

To assess whether biofeedback could effectively modulate SL in healthy subjects, we inspected the distribution of SL_0 values at different gait speeds, reported in Fig. 2. The change in mean SL_0 values at each speed was equal to $\pm 14\%$ in the modulated SL biofeedback conditions, close to the cued $\pm 17\%$ value. Since the maximum standard deviation of the distribution of SL_0 values within each biofeedback condition was relatively small ($\sigma_{MAX} = 7\%$ of the ss-SL_0 values), we concluded that the conducted protocol could significantly modulate values of GS and SL to allow subsequent statistical analysis.

We found a strong relationship ($r = 0.9$) between SL and TLA, which demonstrates that, although not explicitly asked to modulate TLA, subjects did indeed modulate also TLA to match biofeedback-cued SL data. Group analysis of joint torques measured in different SL and GS conditions is shown in Fig. 3.

B. PCA analysis

GS had a strong effect on overall normalized PCA scores $\tilde{a}_i$ ($p < 0.001$ for all joints), while SL had a significant effect only on the hip ($F_{(2,16)} = 4.205$, $p = 0.034$), and knee ($F_{(2,16)} = 28.650$, $p < 0.001$) joint, while no significant

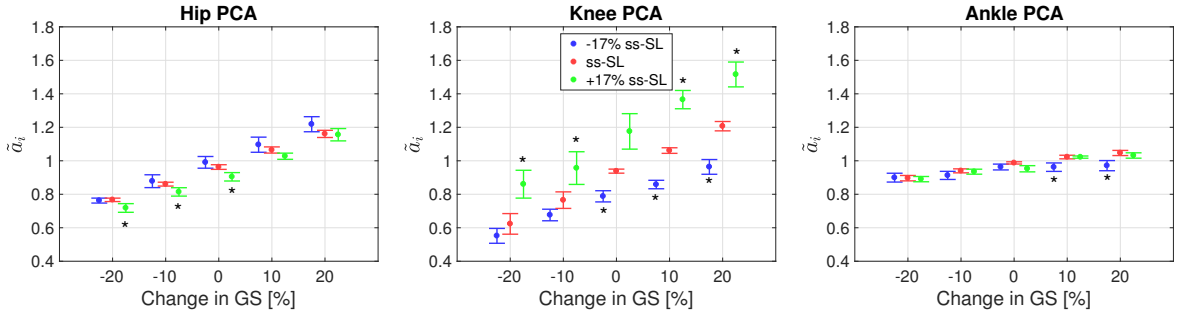

Fig. 4. Distribution of normalized PCA coefficients, as a function of GS, for different SL conditions. Dots in the error bars indicate group mean, with whiskers extending one standard deviation above and below. Asterisks indicate pairwise comparisons between scores extracted at each GS and modulated SL, and scores extracted at the same GS, ss-SL, which are significant at the uncorrected $p < 0.05$ significance level.

effect on the PCA scores was measured for the ankle joint ($F_{(2,16)} = 2.175$, $p = 0.146$). The interaction between SL and GS was significant for the knee joint ($F_{(8,64)} = 2.248$, $p = 0.035$) and the ankle joint ($F_{(8,64)} = 3.062$, $= p-0.006$), while not significant for the hip joint ($F_{(8,64)} = 0.695$, $p = 0.694$). Mean and standard deviation of $\tilde{a}$ parameters calculated for each combination of GS and SL are reported in Fig. 4. Pairwise comparisons between $\tilde{a}_i$ scores measured in self-selected and modulated SL conditions, for all joints, at each speed, yield statistically significant values in 12 out of 20 cases, 7 for the positive modulation of SL, and 5 for the negative modulation of SL. Four comparisons of PCA scores for a positive modulation of SL involve the knee joint, all showing an increase in PCA scores related to an increase in SL (Fig. 4, center). All pairwise comparisons significant for the hip joint are for a positive increase in SL, and show a reduction in hip PCA scores following an increase of SL, all at low speed (Fig. 4, left). The remaining two significant comparisons involve the ankle joint, all at GS values higher than self-selected (Fig. 4, right).

C. Torque pulse approximation

The distributions of parameters pulse time α and pulse amplitude A for each joint are shown in Fig. 5. The most consistent effects of SL were observed in the knee joint, with 70% of pulses occurring between 10% and 20% of the gait cycle. This yielded a distribution of α values for the knee joint whose standard deviation was significantly smaller than the one measured for parameters referring to both the hip and the ankle joint ($\sigma_{\alpha,\text{hip}} = 30\%$ $\sigma_{\alpha,\text{knee}} = 13\%$, $\sigma_{\alpha,\text{ankle}} = 15\%$; Levene's test $F = 15.036$, $p < 0.001$ for the hip vs. knee comparison, $F = 36.138$, $p < 0.001$ for the knee vs. ankle comparison). Analysis of the distribution of parameters A showed the strongest effect on the knee joint ($\mu_{A,\text{hip}} = 0.07$, $\mu_{A,\text{knee}} = 0.26$, $\mu_{A,\text{ankle}} = -0.02$), with both pairwise comparisons with the knee joint significant at the $p < 0.05$ level.

IV. DISCUSSION AND CONCLUSIONS

We used inverse-dynamics to estimate lower extremity joint torques in individuals exposed to a factorial modulation of gait speed (GS), and stride length (SL). Our analysis focused on the estimate of the effect of SL at different values of GS, and showed that the factor SL has a strong effect on the joint torque applied about the knee joint, and a smaller effect about the hip and ankle joint.

Via our PCA analysis and our torque pulse approximation method, we estimated that the primary effect of SL modulation on the knee joint torque profile was that of greater knee flexion torque applied at early stance, i.e. between 10% and 20% of the gait cycle. A secondary effect of SL on knee joint torque was that of an increased knee extension torque during the double support phase of stance. Both effects imply a positive relationship between the increase in knee joint torque applied during normal walking, in those two phases, and the modulation in SL. As such, the knee joint torque in SL-amplified or attenuated conditions is obtained, respectively, by amplifying or attenuating the knee joint torque profile measuring during self-selected (ss) conditions. This effect was captured by PCA of the knee joint torque profile, and by the strong positive effect of SL on knee PCA scores (Fig. 4, center).

An effect of SL was observed at the hip joint. While the reduced SL condition did not result in hip joint torque profiles that differed significantly from the natural SL condition, the PCA scores extracted in the increased SL condition were smaller than in the other two conditions. As such, it appears that increases in SL are obtained by attenuation of the nominal hip joint torque profile, although this effect was statistically significant only at low speeds (Fig. 4 - left).

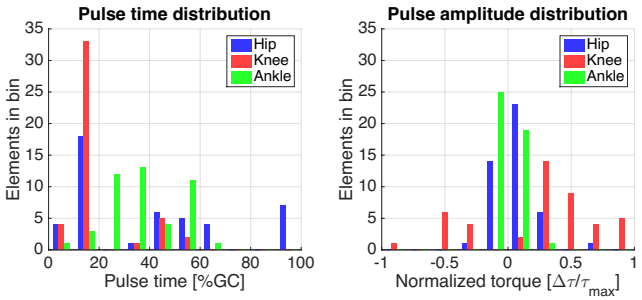

Fig. 5. Distribution of parameters pulse time α (left) and pulse amplitude A (right) extracted via the one pulse approximation method.

A strong effect of SL on hip joint torque was observed at early swing (Fig. 3). Since torques during swing are smaller in amplitude than those measured during stance, analysis methods such as PCA and torque pulse approximation are not sensitive enough to capture the effect of any factor on joint torques measured during swing. Continuum analysis methods, such as the one recently developed in [20], could instead test the statistical significance of the effect of SL on the hip joint torque at early swing, as appears from visual inspection of (Fig. 3, top row central column). As in the case of knee joint torque during stance, the effect of SL on the hip joint torque during early swing was that of a positive increase in hip joint torque with positive increases in SL.

Surprisingly, while ankle torque was strongly modulated by GS, the effect of SL was small, and mostly affecting the negative power, shock absorption phase at early stance. During the instant of peak plantarflexion torque, instead, slight differences in torque profiles were measured, and mostly caused by the -17% SL condition requiring smaller ankle torque compared to the other two conditions. Our finding is in agreement with a previous observation showing that push-off posture is strictly related to propulsive force, and more so than ankle torque at push-off [4].

While we are interested in the development of TLA-oriented robotic gait training strategies, we here investigated joint torques occurring during the modulation of GS and SL, not of GS and TLA. Our analysis showed a strong correlation ($r = 0.9$) between SL and TLA, which demonstrated that, in our protocol, subjects indirectly modulated TLA, even without being explicitly cued to do so.

A limitation of this study resides in the analysis methods used. While PCA and the pulse torque approximation describe the overall effect of an experimental factor (in this case SL), they are not sufficiently fine-grained to capture local effects, i.e. modulation of joint torque profiles in selected phases of the gait cycle. In our future work, we will extend our analysis methods to 1D continuum analysis techniques that allow statistically accurate instant-by-instant comparison of the measured joint torque profiles. Based on the results of these techniques, we will be able to tell *when*, within a gait cycle, the effect of SL on the torque measured in a given joint is greatest, and whether the effect is statistically significant.

Analysis of biofeedback-modulated gait of healthy subjects can only provide inspiration for the design of robotic assistance strategies for gait training. The response of individuals to robotic perturbations, such as those extracted with the pulse torque approximation analysis described in this paper, can not be predicted accurately given the limited understanding of the neuromuscular response to perturbations during gait. Future work will involve human-in-the-loop experiments which will seek to determine which of the extracted robotic perturbation strategies effectively modulates SL and TLA in healthy subjects, as well as in individuals with chronic stroke-induced hemiparesis.

REFERENCES

[1] A. S. Go, D. Mozaffarian, V. L. Roger *et al.*, "Heart Disease and Stroke Statistics–2014 Update: A Report From the American Heart Association," *Circulation*, vol. 129, no. 3, pp. e28–e292, Jan. 2014.

[2] A. Schmid, P. W. Duncan, S. Studenski *et al.*, "Improvements in Speed-Based Gait Classifications Are Meaningful," *Stroke*, vol. 38, no. 7, pp. 2096–2100, Jun. 2007.

[3] M. G. Bowden, C. K. Balasubramanian, R. R. Neptune *et al.*, "Anterior-Posterior Ground Reaction Forces as a Measure of Paretic Leg Contribution in Hemiparetic Walking," *Stroke*, vol. 37, no. 3, pp. 872–876, Feb. 2006.

[4] H. Hsiao, B. A. Knarr, J. S. Higginson *et al.*, "Mechanisms to increase propulsive force for individuals poststroke," *Journal of NeuroEngineering and Rehabilitation*, pp. 12–40, 2015.

[5] J. Mehrholz and M. Pohl, "Electromechanical-assisted gait training after stroke: A systematic review comparing end-effector and exoskeleton devices," *Journal Of Rehabilitation Medicine*, vol. 44, no. 3, pp. 193–199, Mar. 2012.

[6] L. L. Cai, A. J. Fong, C. K. Otoshi *et al.*, "Implications of Assist-As-Needed Robotic Step Training after a Complete Spinal Cord Injury on Intrinsic Strategies of Motor Learning," *Journal of Neuroscience*, vol. 26, no. 41, pp. 10 564–10 568, Oct. 2006.

[7] S. Banala, S. H. Kim, S. Agrawal *et al.*, "Robot Assisted Gait Training With Active Leg Exoskeleton (ALEX)," *Neural Systems and Rehabilitation Engineering, IEEE Transactions on*, vol. 17, no. 1, pp. 2–8, 2009.

[8] A. Duschau-Wicke, J. von Zitzewitz, A. Caprez *et al.*, "Path Control: A Method for Patient-Cooperative Robot-Aided Gait Rehabilitation," *IEEE Transactions on Neural Systems and Rehabilitation Engineering*, vol. 18, no. 1, pp. 38–48, 2010.

[9] B. Koopman, E. H. F. Van Asseldonk, and H. van der Kooij, "Journal of Biomechanics," *Journal of Biomechanics*, vol. 47, no. 6, pp. 1447–1458, Apr. 2014.

[10] R. Ronsse, N. Vitiello, T. Lenzi *et al.*, "Human–robot synchrony: flexible assistance using adaptive oscillators," *IEEE Transactions on Biomedical Engineering*, vol. 4, pp. 1001–1012, 2011.

[11] H. Vallery, E. H. F. Van Asseldonk, M. Buss *et al.*, "Reference Trajectory Generation for Rehabilitation Robots: Complementary Limb Motion Estimation," *IEEE Transactions on Neural Systems and Rehabilitation Engineering*, vol. 17, no. 1, pp. 23–30, Nov. 2009.

[12] T. Yan, A. Parri, V. R. Garate *et al.*, "An oscillator-based smooth real-time estimate of gait phase for wearable robotics," *Autonomous Robots*, pp. 1–16, May 2016.

[13] R. H. Miller, R. Chang, J. L. Baird *et al.*, "Variability in kinematic coupling assessed by vector coding and continuous relative phase," *Journal of Biomechanics*, vol. 43, no. 13, pp. 2554–2560, Sep. 2010.

[14] J. Ahn and N. Hogan, "Walking Is Not Like Reaching: Evidence from Periodic Mechanical Perturbations," *PLoS ONE*, vol. 7, no. 3, p. e31767, Mar. 2012.

[15] M. D. Latt, H. B. Menz, V. S. Fung *et al.*, "Walking speed, cadence and step length are selected to optimize the stability of head and pelvis accelerations," *Exp Brain Res*, vol. 184, no. 2, pp. 201–209, Aug. 2007.

[16] A. L. Hof, "Scaling gait data to body size," *Gait & Posture*, vol. 4, no. 3, pp. 222–223, May 1996.

[17] P. A. Kramer and I. Sarton-Miller, "The energetics of human walking: Is Froude number (Fr) useful for metabolic comparisons?" *Gait & Posture*, vol. 27, no. 2, pp. 209–215, Feb. 2008.

[18] R. Alexander, "The gaits of bipedal and quadrupedal animals," *The International Journal of Robotics Research*, 1984.

[19] T. C. Pataky, J. Vanrenterghem, and M. A. Robinson, "Journal of Biomechanics," *Journal of Biomechanics*, vol. 49, no. 9, pp. 1468–1476, Jun. 2016.

[20] T. C. Pataky, J. Vanrenterghem, and M. A. Robinson, "Zero-vs. one-dimensional, parametric vs. non-parametric, and confidence interval vs. hypothesis testing procedures in one-dimensional biomechanical trajectory," *Journal of Biomechanics*, vol. 48, no. 7, pp. 1277–1285, May 2015.